BJP British Journal of Pharmacology

DOI:10.1111/bph.12457
www.brjpharmacol.org

RESEARCH PAPER

Melatonin MT_1 and MT_2 receptors display different molecular pharmacologies only in the G-protein coupled state

Céline Legros[1], Séverine Devavry[1,2,3], Sarah Caignard[1], Clémence Tessier[1]*, Philippe Delagrange[4], Christine Ouvry[1], Jean A Boutin[1] and Olivier Nosjean[1]

[1]*Biotechnologies, Pharmacologie Moléculaire et Cellulaire, Institut de Recherches Servier, Croissy-sur-Seine, France,* [2]*INRA, UMR85 Physiologie de la Reproduction et des Comportements, Nouzilly, France,* [3]*CNRS, UMR6175, Nouzilly, France, and* [4]*Unité de Recherches en Neurosciences, Institut de Recherches Servier, Croissy-sur-Seine, France*

Correspondence
Jean A Boutin, Biotechnologies, Pharmacologie Moléculaire et Cellulaire, 125 chemin de ronde, Institut de Recherches Servier, F-78290 Croissy-sur-Seine, France.
Email: jean.boutin@fr.netgrs.com

*Present address: Respiratory Disease Area, Novartis Pharmaceuticals UK Limited Horsham UK-RH12 5AB, UK.

Keywords
melatonin; [3H]-melatonin; melatonin receptors; coupling state; GTPγS

Received
10 June 2013
Revised
13 September 2013
Accepted
18 September 2013

BACKGROUND AND PURPOSE

Melatonin receptors have been extensively characterized regarding their affinity and pharmacology, mostly using 2-[^{125}I]-melatonin as a radioligand. Although [^{3}H]-melatonin has the advantage of corresponding to the endogenous ligand of the receptor, its binding has not been well described.

EXPERIMENTAL APPROACH

We characterized [^{3}H]-melatonin binding to the hMT_1 and hMT_2 receptors expressed in a range of cell lines and obtained new insights into the molecular pharmacology of melatonin receptors.

KEY RESULTS

The binding of [^{3}H]-melatonin to the hMT_1 and hMT_2 receptors displayed two sites on the saturation curves. These two binding sites were observed on cell membranes expressing recombinant receptors from various species as well as on whole cells. Furthermore, our GTPγS/NaCl results suggest that these sites on the saturation curves correspond to the G-protein coupled and uncoupled states of the receptors, whose pharmacology was extensively characterized.

CONCLUSIONS AND IMPLICATIONS

hMT_1 and hMT_2 receptors spontaneously exist in two states when expressed in cell lines; these states can be probed by [^{3}H]-melatonin binding. Overall, our results suggest that physiological regulation of the melatonin receptors may result from complex and subtle mechanisms, a small difference in affinity between the active and inactive states of the receptor, and spontaneous coupling to G-proteins.

Abbreviation

2IMLT, 2-iodomelatonin; EC_{50}, radioligand concentration at 50% of the maximum effect; K_D, dissociation constant, B_{max}, maximum binding of the radioligand

Introduction

Melatonin, a hormone mainly synthesized and released by the pineal gland, is well known for its role in the control of mammalian biological rhythms; its known functions now span the biological spectrum from immunology to neuroprotection and depression (see Zawilska *et al.*, 2009; Dubocovich *et al.*, 2010). Melatonin receptors have been identified in

numerous species (Morgan *et al.*, 1994; Williams *et al.*, 1995; 1999; Mazzucchelli *et al.*, 1996; Drew *et al.*, 2001). Two receptors have been cloned in humans, hMT_1 and hMT_2 and have been characterized as seven-transmembrane GPCRs (receptor nomenclature follows Alexander *et al.*, 2013). These receptors bind melatonin with high affinity (20–200 pM) and are both mainly coupled to the inhibition of adenylyl cyclase (Reppert *et al.*, 1994; Reppert *et al.*, 1995; Masana and Dubocovich, 2001). Like most GPCRs, the cellular signalling of hMT_1 and hMT_2 receptors occurs via the recruitment of G-proteins and/or β-arrestin, and can be further modulated by other mechanisms, including allosterism and receptor homo- and heterodimerization as the most common mechanisms. For instance, melatonin receptors have been described as homo- and heterodimers when expressed in cellular systems (Ayoub *et al.*, 2002).

The main radioligand used to study the melatonin receptors is 2-[^{125}I]-melatonin (Vakkuri *et al.*, 1984). With its high affinity for MT_1 and MT_2 receptors and its high specific activity, use of this radioligand enabled the description of the distribution of melatonin receptors in many organs and species (see Jockers *et al.*, 2008), the characterization of the receptors in cellular systems, and the identification of a large range of agonists and antagonists (Witt-Enderby and Dubocovich, 1996; Nonno *et al.*, 1998; Audinot *et al.*, 2003; 2008; Zlotos *et al.*, 2009). [^{3}H]-melatonin, which is structurally identical to the natural ligand of the melatonin receptors, is an interesting alternative radioligand, although its lower specific activity has sometimes limited its applicability, especially for binding to tissue sections that express the melatonin binding sites at very low density. Interestingly, the overall pharmacology of [^{3}H]-melatonin compares well that of with 2-[^{125}I]-melatonin, although there are not many reports describing the pharmacology of the tritiated ligand (Niles, 1987; Kennaway *et al.*, 1994; Browning *et al.*, 2000).

Here, we report a comparative description of the molecular pharmacologies of hMT_1 and hMT_2 using these two radioligands. Our study confirms our recent findings that hMT_1 and hMT_2 are spontaneously expressed, as being pre-coupled to G-proteins (Devavry *et al.*, 2012b), and that it is in this state that the receptors exhibit different pharmacologies; they have the same ligand-binding properties when they are un-coupled from G-proteins.

Methods

Membrane preparation

CHO-K1, HEK293 and Neuro2A cell lines stably expressing the MT_1 or MT_2 receptor (of human, rat, mouse, or sheep) were grown to confluence, harvested in PBS (Gibco, Invitrogen, Paisley, UK) containing 5 mM EDTA, and centrifuged at 1000× *g* for 20 min (4°C). The resulting pellet was resuspended in 5 mM Tris/HCl [pH 7.4] containing 2 mM EDTA, and was homogenized using a Kinematica polytron (Kinematica AG, Luzern, Switzerland). The homogenate was then centrifuged (20 000× *g*, 30 min, 4°C), and the resulting pellet was resuspended in 75 mM Tris/HCl [pH 7.4] containing 2 mM EDTA and 12.5 mM $MgCl_2$. Determination of protein content was performed according to the Bradford method (Bradford, 1976) using the Bio-Rad DC™ Protein Assay Kit (Bio-Rad SA, Ivry-sur-Seine, France). Aliquots of membrane preparations were stored in re-suspension buffer (75 mMTris/HCl [pH 7.4], 2 mM EDTA, 12.5 mM $MgCl_2$) at –80°C until use.

[^{3}H]-melatonin and 2-[^{125}I]-melatonin membrane-binding assay

Radioligand binding assays were performed in 96-well plates in a final volume of 250 µL in binding buffer (Tris/HCl 50 mM [pH 7.4], 5 mM $MgCl_2$, 1 mM EDTA). Membranes, hMT_1 and hMT_2, were used at a final concentration of 30 µg·mL^{-1}. Non-specific binding was defined with 10 µM melatonin. The reaction was stopped by rapid filtration through GF/B unifilters (PerkinElmer, Waltham, MA, USA) followed by three successive washes with ice-cold 50 mM Tris/HCl [pH 7.4].

Kinetic parameters (K_{on}, K_{off} and $K_{Dkinetics}$) of [^{3}H]-melatonin and 2-[^{125}I]-melatonin were measured on hMT_1 and hMT_2 at 37°C and at room temperature. For association studies, membranes were added to [^{3}H]-melatonin (0.6 nM) and incubated for increasing periods of time (5–360 min). For dissociation studies, membranes were incubated with [^{3}H]-melatonin (0.6 nM) for 20 min, 1 h or 3 h prior to the addition of cold melatonin (10 µM) to initiate dissociation, and then incubated for increasing periods of time (0–240 min). For 2-[^{125}I]-melatonin association studies, membranes were added to 2-[^{125}I]-melatonin (0.025 nM) and incubated for increasing periods of time (5–360 min). For dissociation studies, membranes were incubated with 2-[^{125}I]-melatonin (0.025 nM) for 20 min and 2 h prior to the addition of cold melatonin (10 µM) to initiate dissociation, and then incubated for increasing periods of time (0–120 min). Kinetic measurements were repeated at least twice on the same pool of membranes to the limit of membrane availability.

Saturation experiments with [^{3}H]-melatonin were performed in the equilibrium state, as determined from kinetics experiments. Membranes were incubated for 2 h (for hMT_1) or 3 h (for hMT_2) at 37°C in binding buffer containing [^{3}H]-melatonin (0.01–20 nM). Saturation experiments with 2-[^{125}I]-melatonin were also performed at equilibrium, with cellular membranes incubated for 2 h at 37°C in binding buffer containing 2-[^{125}I]-melatonin (0.02–2.0 nM) as described previously (Audinot *et al.*, 2003).

For competition studies, membranes were first incubated in binding buffer with compounds (10^{-15} to 10^{-5} M final, DMSO 1% final) for 1 h (hMT_1) or 2 h (hMT_2) at 37°C, and then incubated with [^{3}H]-melatonin (5 nM) for 1 more hour for hMT_1 and 2 more hours for hMT_2 at 37°C. Non-specific binding was defined with 10 µM melatonin. The reaction was stopped by rapid filtration through GF/B unifilters, followed by three successive washes with ice-cold 50 mM Tris/HCl [pH 7.4].

G-protein uncoupling conditions were achieved by pre-incubating the cellular membranes for 30 min at 37°C with 100 µM GTPγS and 350 mM NaCl for hMT_1 and with 100 µM GTPγS and 700 mM NaCl for hMT_2. The incubated solutions were then added to [^{3}H]-melatonin or 2-[^{125}I]-melatonin for saturation tests or competition tests according to the protocols described above. In control conditions, membranes were pre-incubated with binding buffer for 30 min at 37°C.

Experiments with suspended cells

CHO-K1 cells stably expressing the hMT_1 or hMT_2 receptor were grown to confluence, harvested in PBS containing 5 mM EDTA, and centrifuged at 100× *g* for 10 min (4°C). The resulting pellet was suspended in HBSS (Gibco), and cells were counted using Vi-Cell (Beckman Coulter, Villepinte, France). From a previously sonicated cell sample, total protein concentration was measured according to the Bradford method using the Bio-Rad DC™ Protein Assay Kit (Bio-Rad SA, Ivry-sur-Seine, France). Cells were diluted in HBSS to a final condition of 25 000 cells in 200 µL. Binding experiments used the same protocols as the membrane-binding experiments. All binding reagents (cells, radioligand and compound) were diluted in HBSS buffer. For saturation experiments, hMT_1- and hMT_2-expressing cells were incubated for 1 h at 37°C with [^{3}H]-melatonin (0.01–20.0 nM). For competition assays, cells were co-incubated with ligands (10^{-15} to 10^{-5} M) and [^{3}H]-melatonin (1 nM for hMT_1; 0.5 nM for hMT_2). Non-specific binding was defined with 10 µM melatonin. The reaction was stopped by rapid filtration through GF/B unifilters, followed by three successive washes with ice-cold 50 mM Tris/HCl [pH 7.4].

Data analysis

Data were analysed using PRISM 5.04 (GraphPad software Inc., San Diego, CA, USA). For saturation assays, the number of maximum binding sites (B_{max}) and the dissociation constant of the radioligand (K_D) were calculated according to the method of Scatchard (Acuna-Castroviejo *et al.*, 1994). For each saturation experiment, nonlinear regression data were statistically analysed by extra-sum of squares *F*-test (PRISM 5.04, GraphPad software) to test the hypothesis of preferred fitting model of the regression curve, one or two sites (one site regression curve equation: $Y = B_{max} \times X/(K_D + X)$; two sites regression curve equation: $Y = B_{max1} \times X/(K_{D1} + X) + B_{max2} \times X/(K_{D2} + X)$. Association kinetic data were analysed by fitting specific binding data to the equation $B = B_{max} \times (1\text{-}\exp^{(-k \times t)})$, where *B* is binding at time t and k is the observed association rate constant. Dissociation kinetic data were analysed by fitting specific binding to the equation $B = B_{max} \times \exp^{(-k+t)}$ + plateau, where k is the dissociation rate constant. The extra-sum of squares *F*-test (PRISM 5.04, GraphPad software) was also used to determine the preferred regression model, one or two sites, in kinetics experiments. Kinetic K_D was calculated as $K_{Dkinetics} = k_{off}/k_{on}$, with k_{off} representing the dissociation constant (s^{-1}) and K_{on} ($M^{-1} \cdot s^{-1}$) representing the association constant; kinetic K_D is expressed as $pK_D = -\log(K_D)$. For competition experiments, inhibition constants (K_I) were calculated according to the Cheng–Prusoff equation (Cheng and Prusoff, 1973): $K_I = IC_{50}/[1 + (L/K_D)]$, where IC_{50} is the 50% inhibition concentration, L is the concentration of [^{3}H]-melatonin and K_D the K_D of the high-affinity site. K_D and K_I values are expressed as pK_D and pK_I, with $pK_D = -\log(K_D)$ and $pK_I = -\log(K_I)$. The Pearson product–moment correlation coefficient was employed for correlation analysis of pK_I values.

Materials

[^{3}H]-melatonin (specific activity 80–85 Ci·mmol^{-1} – 3 atoms of tritium per melatonin molecule) was purchased from American Radiolabeled Chemicals Inc. (St Louis, MO, USA) and

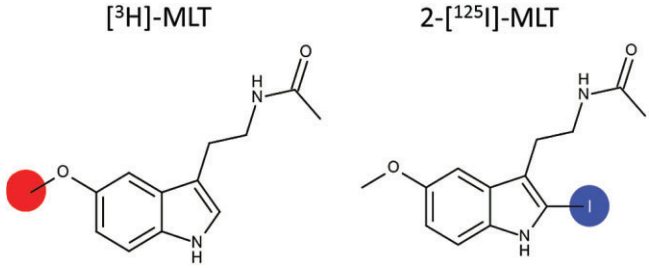

Figure 1

[^{3}H]-melatonin ([^{3}H]-MLT) and 2-[^{125}I]-melatonin (2-[^{125}I]-MLT) chemical structures. Labelling position in red for the [^{3}H]-MLT and in blue for the 2-[^{125}I]-MLT.

2-[^{125}I]-melatonin (specific activity 2200 Ci·mmol^{-1}) was purchased from Perkin Elmer (Boston, MA, USA). Radioligand structures and labelling position are illustrated in Figure 1. Melatonin, 2-iodo-melatonin, 6-chloromelatonin, 5-HT and D 600 (+/– methoxy verapamil) were obtained from Sigma (St Louis, MO, USA); 4-phenyl-2-propionamidotetraline and luzindole (2-benzyl-N-acetyltryptamine) were purchased from Tocris (Bristol, UK), and 2-bromomelatonin was purchased from Toronto Research Chemicals Inc. (Toronto, Canada). We evaluated 15 analogues of melatonin from our product library whose structures are available in Depreux *et al.*, 1994; Audinot *et al.*, 2003; Mailliet *et al.*, 2004; Audinot *et al.*, 2008; Devavry *et al.*, 2012a; Devavry *et al.*, 2012b; Legros *et al.*, 2013 and Ettaoussi *et al.*, 2013. Compounds were dissolved in DMSO at a stock concentration of 10 mM and stored at –20°C until use. All other reagents were obtained from Sigma.

Results

Association and dissociation kinetics

The hMT_1 and hMT_2 receptors exhibited different kinetic profiles (Figure 2), with a slightly slower profile for hMT_2 that reflected little or any dissociation of [^{3}H]-melatonin; for hMT_1, association was fast and the dissociation was total or nearly total (Figure 2). At 37°C, hMT_1 showed one-component association fast kinetics, and hMT_2 exhibited a two-parameter kinetic association. The binding plateau was reached in 30 min for hMT_1 and in 90 min for hMT_2. Kinetic parameters (k_{on}, k_{off}, $K_{Dkinetics}$ and $t_{1/2}$s) are described in Table 1. Kinetics were 2–5 times slower at room temperature than at 37°C, and both receptors displayed a two-parameter association profile. In addition, dissociation from hMT_1 was only partial, and no dissociation of the radioligand was observed from hMT_2.

The association and dissociation kinetics of 2-[^{125}I]-melatonin (Figure 3) were slower than those of [^{3}H]-melatonin on the hMT_1 and hMT_2 receptors. The half-time of association at 37°C was 10 times slower than that for [^{3}H]-melatonin: 20.5 min for hMT_1 and 36.4 min for hMT_2 (plateau was reached in 2 h for hMT_1 and in ~4 h for hMT_2). The half-association times doubled when the association reaction was run at room temperature. For both receptors, dissociation was only partial at 37°C for the two dissociation

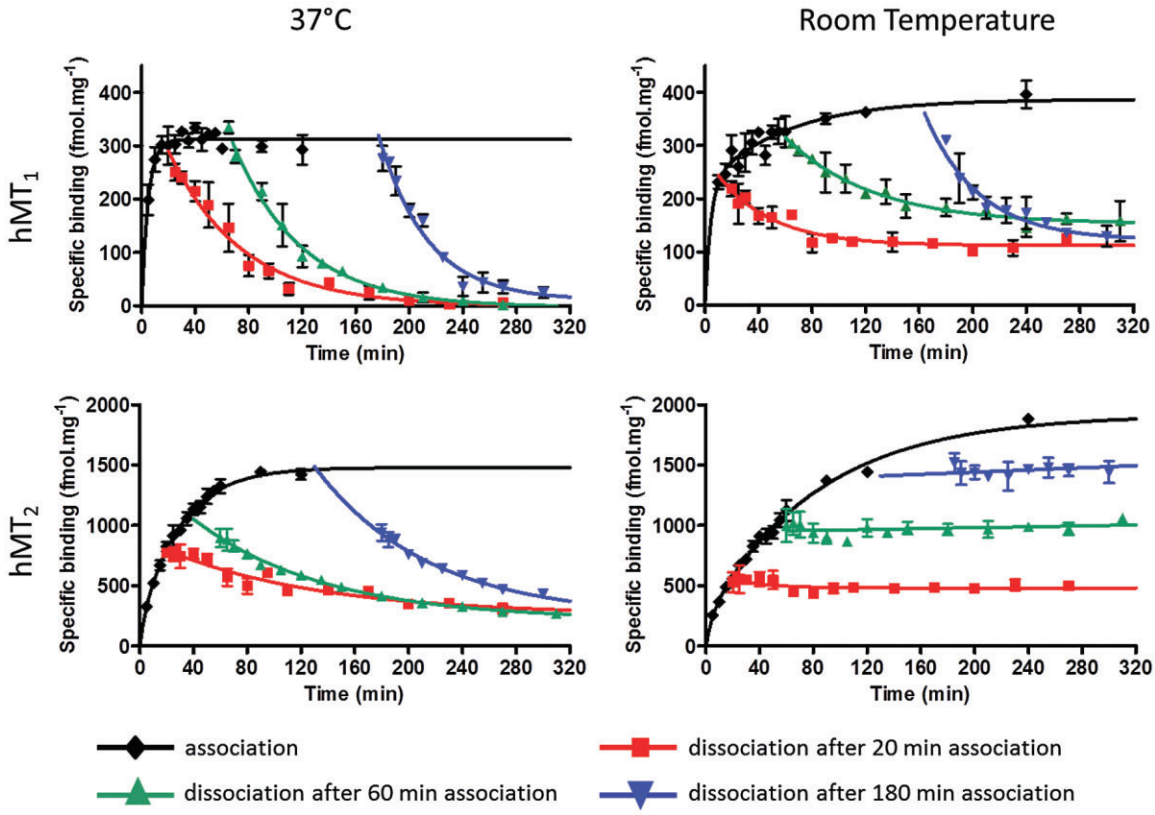

Figure 2

Time course of association and dissociation of [^{3}H]-melatonin (0.6 nM) binding to hMT$_1$ and hMT$_2$ receptors at 37°C and at room temperature. Dissociation was measured at three association times (20 min; 60 min and 180 min). Data are the mean (±SEM) of at least two experiments at the same time points.

times, and no dissociation was measurable at room temperature. The kinetic parameters (k_{on}, k_{off}, $K_{Dkinetics}$ and $t_{1/2}$s) are shown in Table 1.

Saturation isotherms for hMT$_1$ and hMT$_2$ receptors

CHO-hMT$_1$ and CHO-hMT$_2$ membrane preparations were characterized by 2-[^{125}I]-melatonin binding and showed classical high-affinity values, with pK_D = 10.64 ± 0.11 for hMT$_1$ receptors (mean ± SEM, n = 5) and pK_D = 10.11 ± 0.05 for hMT$_2$ receptors (mean ± SEM, n = 8; Figure 4). Interestingly, [^{3}H]-melatonin experiments yielded saturation isotherms that, after Scatchard linearization, clearly showed a biphasic profile for the two receptors, indicating the presence of two different pharmacological sites in the membrane preparations (Figure 4). A high-affinity site (site 1) yielded values of pK_{D1} = 10.23 ± 0.07 for hMT$_1$ and pK_{D1} = 9.87 ± 0.05 for hMT$_2$; a second site (site 2) displayed a lower affinity, with pK_{D2} = 9.46 ± 0.01 for hMT$_1$ and pK_{D2} = 9.26 ± 0.05 for hMT$_2$ (mean ± SEM, n = 12 for for hMT$_1$ and n = 10 for hMT$_2$). Site 1 was five- to sixfold predominant over site 2, with B_{max1} = 574.6 ± 76.7 fmol·mg^{-1} versus B_{max2} = 96.3 ± 11.9 fmol·mg^{-1} for hMT$_1$, and B_{max1} = 2219.9 ± 178.2 fmol·mg^{-1} versus B_{max2} = 462.7 ± 68.3 fmol·mg^{-1} for hMT$_2$. Notably, for both radioligands the maximum number of binding sites was substantially higher for hMT$_2$ than for hMT$_1$ (~2000 vs. ~600 fmol·mg^{-1}, respectively), which is consistent with our experience that MT$_2$ receptors of any species are easier to express in heterologous systems than MT$_1$ receptors.

Exploration of [^{3}H]-melatonin binding across experimental conditions and species

We further documented the binding sites for [^{3}H]-melatonin on the melatonin receptors under various experimental conditions. First, recombinant human receptors were evaluated in live cells, using the same CHO cell lines as were used for the membrane binding experiments. Under these conditions, hMT$_1$, but not hMT$_2$ receptors, showed two binding sites, with the following values: CHO-hMT$_1$: pK_{D1} = 9.61 ± 0.08, pK_{D2} = 8.75 ± 0.16, B_{max1} = 119.9 ± 43.2 fmol·mg^{-1} and B_{max2} = 79.3 ± 17.6 fmol·mg^{-1} (mean ± SEM, n = 4); CHO-hMT$_2$: pKd = 9.43 ± 0.08 and B_{max} = 1192.8 ± 395.1fmol·mg^{-1} (mean ± SEM, n = 5). Under these conditions, 2-[^{125}I]-melatonin displayed a single binding site for CHO-hMT$_1$: pK_D = 10.36 ± 0.05 and B_{max} = 125.1 ± 28.8 fmol·mg^{-1}; CHO-hMT$_2$: pK_D = 9.78 ± 0.27 and B_{max} = 933.0 ± 247.5 fmol·mg^{-1} (mean ± SEM, at least n = 2). Second, we characterized [^{3}H]-melatonin binding to cell membranes with recombinant human melatonin receptors expressed in two other cell lines: human HEK cells of non-neuronal origin, and murine Neuro2A cells of neuronal

Table 1

Kinetic parameters of [^{3}H]-melatonin ([^{3}H]-MLT) and 2-[^{125}I]-melatonin (2-[^{125}I]-MLT) to the hMT_1 and hMT_2 receptors at 37°C and at room temperature (RT)

			$pK_{D(kinetics)}$ (1)	$pK_{D(kinetics)}$ (2)	Association $t_{1/2}$ (l) (min)	Association $t_{1/2}$ (2) (min)	Dissociation $t_{1/2}$ (min)	k_{on}(1) ($M^{-1}.s^{-1}$)	k_{on}(2) ($M^{-1}.s^{-1}$)	k_{off} (s^{-1})
37°C	[^{3}H]-MLT	hMT_1	10.24 ± 0.05	–	3.0 ± 0.6	–	33.6 ± 2.9	6.10×10^6	–	3.54×10^{-4}
		hMT_2	10.72 ± 0.02	9.91 ± 0.02	2.6 ± 0.7	16.6 ± 5.7	69.3 ± 8.2	7.37×10^6	1.13×10^6	1.42×10^{-4}
	2-[^{125}I]-MLT	hMT_1	10.94 ± 0.11	–	20.5 ± 4.2	–	48.6 ± 12.5	2.20×10^7	–	2.55×10^{-4}
		hMT_2	–	–	36.4 ± 4.1	–	–	1.23×10^7	–	–
RT	[^{3}H]-MLT	hMT_1	10.30 ± 0.05	9.08 ± 0.05	2.7 ± 0.7	44.8 ± 2.8	35.0 ± 2.1	6.75×10^6	4.03×10^5	3.37×10^{-4}
		hMT_2	–	–	6.1 ± 3.8	90.3 ± 45.7	–	3.78×10^6	2.35×10^5	–
	2-[^{125}I]-MLT	hMT_1	10.60 ± 0.06	–	48.6 ± 6.7	–	48.6 ± 6.7	9.58×10^6	–	2.41×10^{-4}
		hMT_2	–	–	79.9 ± 9.9	–	–	5.60×10^6	–	–

Kinetic parameters (K_{on}, K_{off}, $t_{1/2}$) of [^{3}H]-melatonin and 2-[^{125}I]-melatonin were measured on membranes from CHO-K1 cells expressing either hMT_1 or hMT_2 receptors. pK_D was calculated as $pK_D = -\log(K_{off}/K_{on})$. Results are given as mean ± SEM for at least two experiments.

origin. In both cases, hMT_1 and hMT_2 receptors consistently exhibited two binding sites upon saturation with tritiated melatonin, with pK_D values very similar to those obtained with CHO cell lines (Table 2; mean ± SEM, n = 2). Third, we evaluated [^{3}H]-melatonin binding to melatonin receptors from sheep (Mailliet *et al.*, 2004; Cogé *et al.*, 2009), mouse (Devavry *et al.*, 2012a) and rat (Audinot *et al.*, 2008), most of which had been initially cloned in our laboratory. Again, in all cases, melatonin receptors expressed in CHO cells displayed a biphasic saturation curve (Table 2; mean ± SEM, n = 2) consistent with the observations from human receptors. Further, our control experiments demonstrated that all naïve cells (CHO, HEK and Neuro2A) were completely devoid of endogenous melatonin binding sites.

These data indicate that human and ovine receptors share the same overall profile, with pK_D values between the two sites differing by a factor of 4–9, and pK_D values differing between MT_1 and MT_2 receptors by a factor of two or less. In addition, the proportion of binding to site 2 versus the total number of maximal binding sites varied from 15 to 30%. The mouse and rat receptors exhibited a different binding profile, with pK_D values between the two sites differing by a factor of two, and pK_D values differing between MT_1 and MT_2 receptors by a factor of 4–8. Furthermore, these receptors displayed a higher proportion of site 2 binding, which accounted for 40% of binding to the overall maximum number of binding sites.

Evaluation of the effect of G-protein uncoupling agents on melatonin binding

We evaluated the hypothesis that binding site 2 represented a different state of activation of the hMT receptors by exploring the effect of G-protein uncoupling agents on the [^{3}H]-melatonin saturation isotherms. GTPγS and NaCl have been reported to decrease the recruitment of G-proteins to GPCRs (Nonno *et al.*, 1998); here we used these reagents with CHO-hMT_1 and CHO-hMT_2 membrane preparations. Our protocol optimization allowed us to determine the appropriate conditions for hMT_1 (100 μM GTPγS and 350 mM NaCl) and for hMT_2 receptors (100 μM GTPγS and 700 mM NaCl). When subjected to GTPγS and NaCl pretreatment, hMT_1 and hMT_2 receptors both showed complete disappearance of the high-affinity binding site 1, to the benefit of the binding site 2; the number of total maximal binding sites remained relatively unchanged (Figure 5, Table 3). The affinity constant (pK_I) for binding site 2 (the lower-affinity site) shifted from 9.24 (hMT_2) and 9.32 (hMT_1) in the absence of uncoupling agent to 8.75 (hMT_2) and 7.82 (hMT_1) in the presence of GTPγS and NaCl. Notably, the apparent affinity of binding site 2 of hMT_1 underwent a stronger shift in the presence of GTPγS and NaCl, which will be discussed later in this report. The effect of GTPγS and NaCl as uncoupling agents was also evaluated on the binding of 2-[^{125}I]-melatonin, which displayed a single binding site under control conditions (Figures 4 and 5, Table 3). Upon treatment of membranes with GTPγS and NaCl, the affinity of the binding site for 2-[^{125}I]-melatonin was decreased by a factor of ~10 for hMT_1 and by a factor of approximately 3 for hMT_2 receptors. The total number of binding sites was conserved for hMT_2 after incubation with the decoupling agents; as for [^{3}H]-melatonin binding, hMT_1 receptors displayed an unexpected decrease in the total

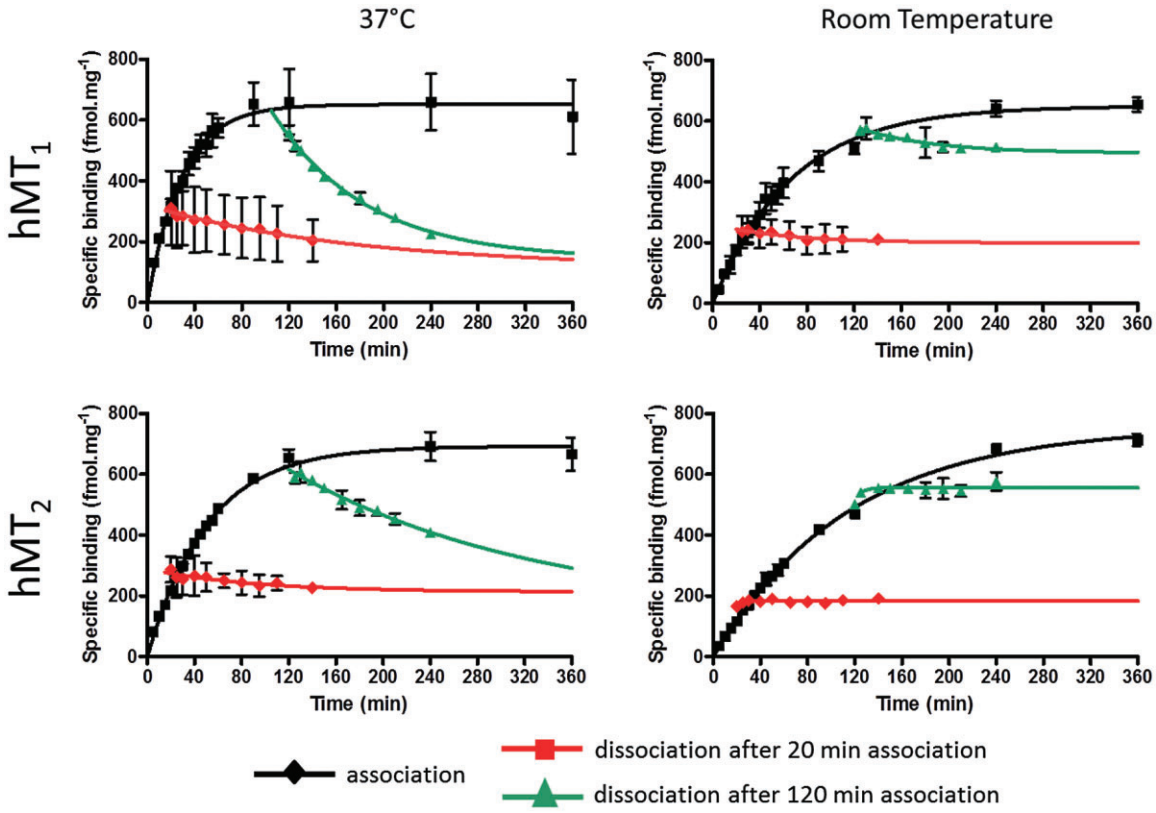

Figure 3

Time course of association and dissociation of 2-[^{125}I]-melatonin (0.025 nM) binding to hMT_1 and hMT_2 receptors at 37°C and at room temperature. Dissociation was measured at two association times (20 min; 120 min). Data are the mean (±SEM) of at least two experiments at the same time points.

Table 2

pK_D and B_{max} of [^{3}H]-melatonin binding to melatonin receptors from various species

	pK_{D1}	pK_{D2}	B_{max1} fmol·mg proteins^{-1}	B_{max2} fmol·mg proteins^{-1}
CHO-hMT_1	10.23 ± 0.07	9.46 ± 0.01	574.6 ± 76.7	96.3 ± 11.9
CHO-hMT_2	9.87 ± 0.05	9.26 ± 0.05	2219.9 ± 178.2	462.7 ± 68.3
HEK293-hMT_1	10.05 ± 0.17	9.30 ± 0.23	544.4 ± 455.7	227.0 ± 176.0
HEK293-hMT_2	9.76 ± 0.12	9.17 ± 0.25	1249.1 ± 1061.9	305.4 ± 145.2
Neuro2A-hMT_1	10.21 ± 0.01	9.38 ± 0.29	133.1 ± 12.0	26.5 ± 7.5
Neuro2A-hMT_2	10.15 ± 0.25	9.52 ± 0.41	484.8 ± 277.3	118.6 ± 61.8
CHO-oMT_1	9.82 ± 0.16	9.04 ± 0.01	1323.5 ± 64.0	546.0 ± 85.0
CHO-oMT_2	9.61 ± 0.09	8.96 ± 0.07	457.6 ± 31.4	158.3 ± 48.2
CHO-mMT_1	9.17 ± 0.08	8.97 ± 0.10	566.2 ± 13.0	356.1 ± 60.7
CHO-mMT_2	9.05 ± 0.16	8.68 ± 0.06	289.2 ± 33.2	96.4 ± 4.4
CHO-rMT_1	9.80 ± 0.14	8.93 ± 0.07	144.3 ± 35.9	94.1 ± 5.9
CHO-rMT_2	9.21 ± 0.01	8.86 ± 0.05	1055.7 ± 393.6	313.4 ± 107.0

hMT_1 and hMT_2 receptors were stably expressed in CHO-K1, Neuro2A and HEK293 cells. Ovine (o), mouse (m) and rat (r) MT_1 and MT_2 receptors were expressed on CHO-K1 cells. Results are given as mean ± SEM for at least two experiments.

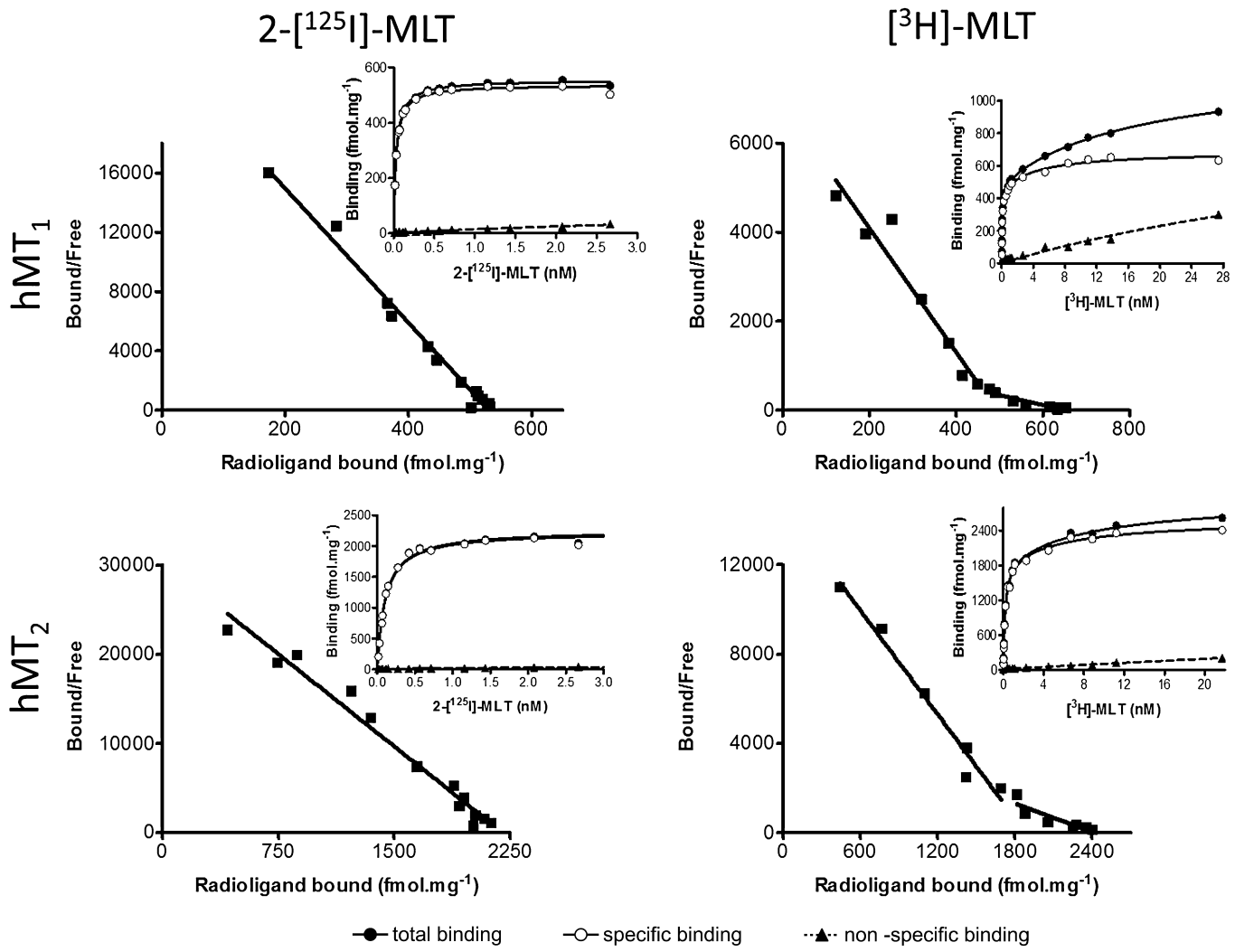

Figure 4

Saturation and Scatchard regression for the hMT_1 and hMT_2 receptors, with 2-[^{125}I]-melatonin (incubation 2 h at 37°C) and [^{3}H]-melatonin (incubation 2 h at 37°C for hMT_1 and 3 h at 37°C for hMT_2). Graphs are representative of all experiments in each case.

Table 3

Comparison of pK_D and B_{max} for binding of [^{3}H]-melatonin ([^{3}H]-MLT) and 2-[^{125}I]-melatonin (2-[^{125}I]-MLT) to the human melatonin receptors

		pK_{D1}	pK_{D2}	B_{max1} fmol·mg proteins^{-1}	B_{max2} fmol·mg proteins^{-1}
[^{3}H]-MLT	hMT_1 control	10.20 ± 0.03	9.32 ± 0.21	982.7 ± 59.2	111.3 ± 34.8
	hMT_2 control	9.77 ± 0.04	9.24 ± 0.04	2794.0 ± 148.9	645.3 ± 73.5
	hMT_1 GTPγS + NaCl	–	7.82 ± 0.07	–	899 ± 97
	hMT_2 GTPγS + NaCl	–	8.75 ± 0.02	–	3768.7 ± 261.3
2-[^{125}I]-MLT	hMT_1 control	10.64 ± 0.11	–	688.9 ± 138.5	–
	hMT_2 control	10.11 ± 0.05	–	2340.6 ± 92.3	–
	hMT_1 GTPγS + NaCl	9.56 ± 0.1	–	245.3 ± 33.0	–
	hMT_2 GTPγS + NaCl	9.56 ± 0.07	–	2617.3 ± 328.5	–

pK_D and B_{max} of [^{3}H]-melatonin and 2-[^{125}I]-melatonin were measured on membranes from CHO-K1 cells expressing either hMT_1 or hMT_2 receptors, in the presence of 100 μM GTPγS and/or 350 mM (hMT_1) or 700 mM (hMT_2) NaCl. Mean ± SEM are given for at least three experiments.

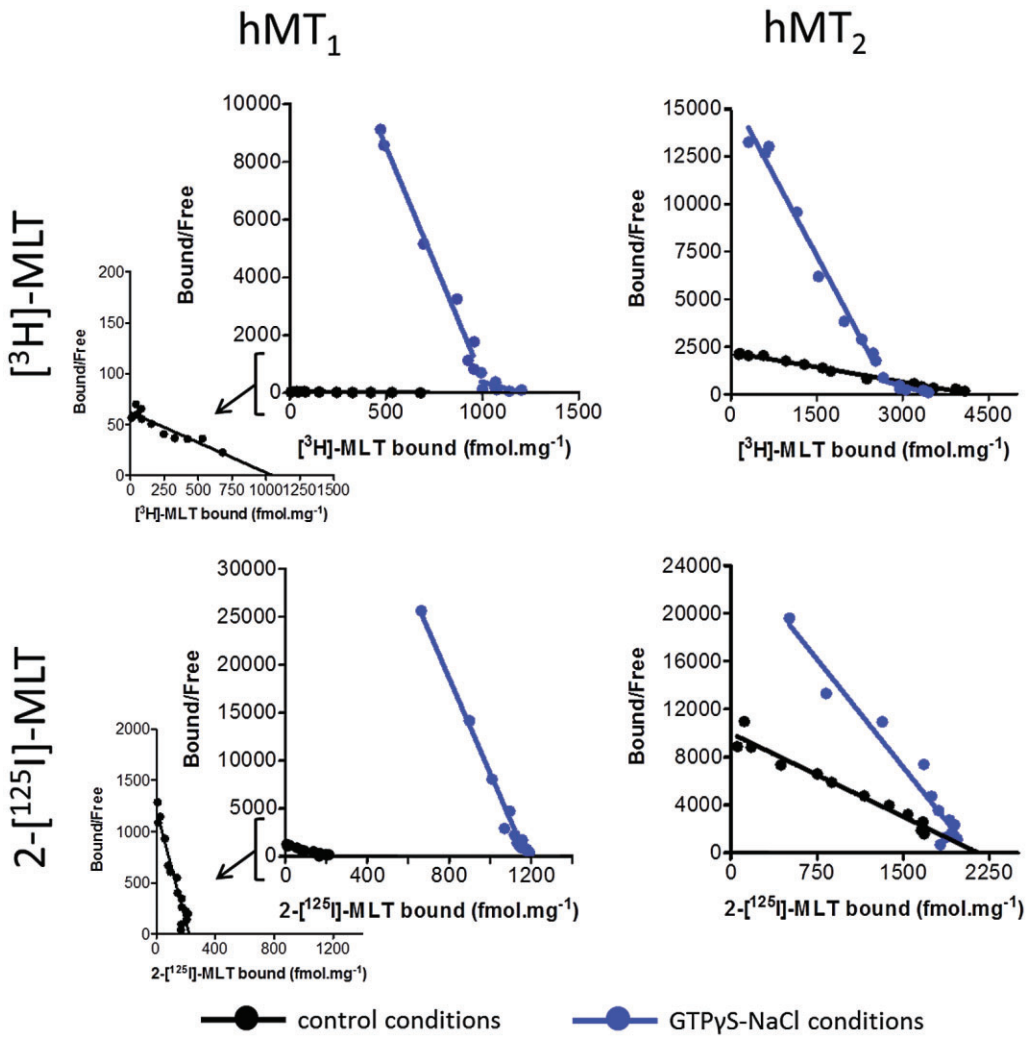

Figure 5

Effect of 100 μM GTPγS and 350 mM NaCl for hMT_1 or 100 μM GTPγS and 700 mM NaCl for hMT_2 in saturation experiments (Scatchard regression) with [^{3}H]-melatonin ([^{3}H]-MLT) or 2-[^{125}I]-melatonin (2-[^{125}I]-MLT). Each curve is representative of all experiments in each case (n = 3).

number of binding sites, by a factor of six in the case of 2-[^{125}I]-melatonin.

Pharmacology

Finally, it was important to evaluate whether these two binding sites exhibit the same pharmacology. We therefore assessed a set of 24 compounds that either already had been described (melatonin derivatives, 4-phenyl-2-propionamidotetraline, luzindole, ramelteon) or had been prepared via medicinal chemistry in our melatonin research programme. These compounds were tested on hMT_1 and hMT_2 receptors, on membrane preparations or live cells, and against 2-[^{125}I]-melatonin or [^{3}H]-melatonin. Under standard, non-uncoupling binding conditions, the binding data all consistently exhibited reasonable to good correlation among the various datasets (Figure 6, Table 4). [^{3}H]-melatonin pharmacology mostly replicated 2-[^{125}I]-melatonin pharmacology, both for hMT_1 and hMT_2 receptors. In addition, radioligand binding to live cells yielded pK_I values that were well correlated with the data obtained from membrane preparations; we detected a slight bias in the correlation in which the difference in potency between the compounds was less important in cells than in membranes. This tendency was clearer with hMT_2 than with hMT_1 receptors (Figure 6).

We then evaluated the pharmacology of these compounds with membrane preparations treated with GTPγS and NaCl. The data obtained with and without the uncoupling agents are represented in Figure 7 and Table 5, where compounds are annotated according to their functional response in a [^{35}S]-GTPγS binding assay. In this comparison, GTPγS and NaCl treatment tended to increase the affinity of inverse agonists and decrease the affinity of agonists. This tendency was more pronounced with hMT_1 than with hMT_2 receptors, and was more visible with [^{3}H]-melatonin than with 2-[^{125}I]-melatonin. This difference of compound behaviour is

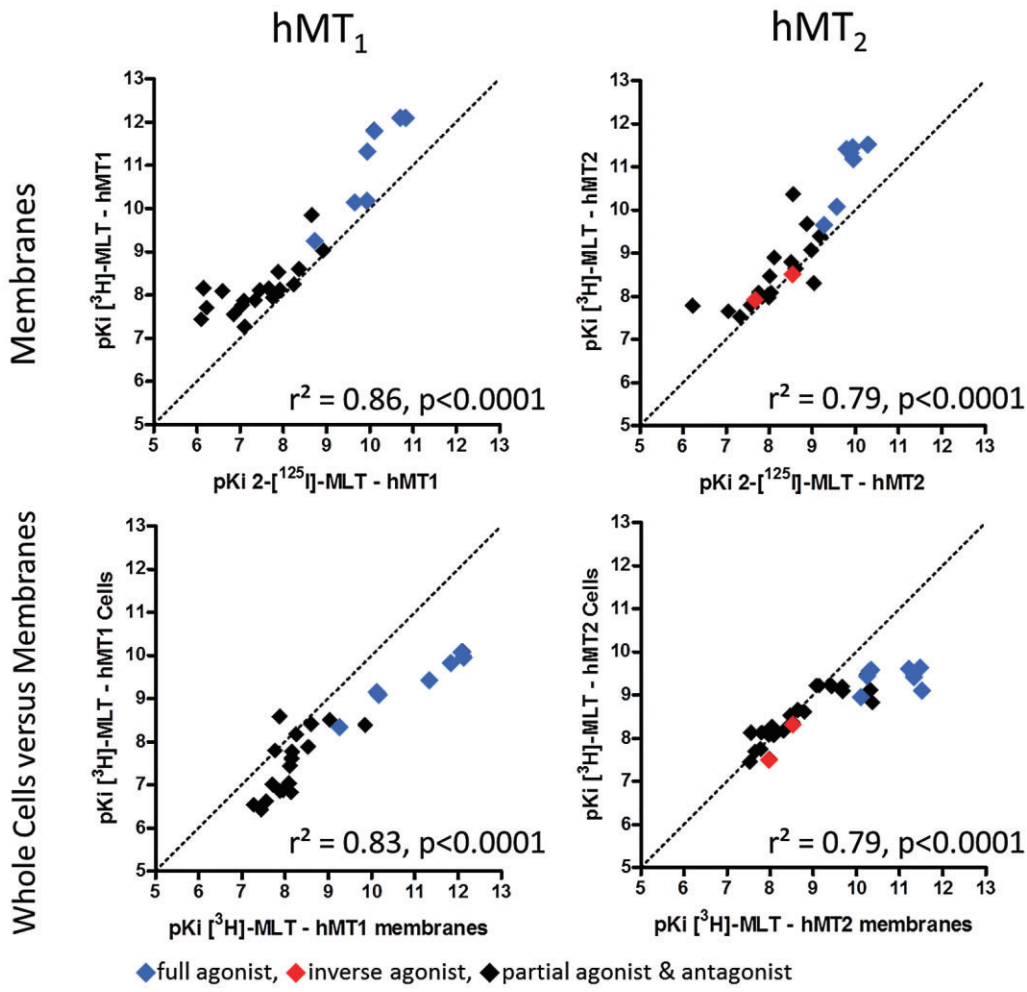

Figure 6

Correlation plots of binding affinities [expressed as $pK_I = -\log(K_I)$] determined for [^{3}H]-melatonin ([^{3}H]-MLT) or 2-[^{125}I]-melatonin (2-[^{125}I]-MLT; from reference database) binding to hMT_1 and hMT_2 receptors in membrane preparations. Correlation plots of binding affinities were generated for [^{3}H]-melatonin binding to hMT_1 and hMT_2 receptors expressed in whole cells or in membrane preparations.

illustrated in Figures 8 and 9, which shows IC_{50} curves for both radioligand in control and uncoupling conditions that reflect the shift of affinity in presence of GTPγS and NaCl.

Discussion

For practical reasons, the molecular pharmacology of the melatonin receptors has traditionally been elucidated using 2-[^{125}I]-melatonin. Use of this radioligand has largely contributed to most of the discoveries made in the melatonin field, including our internal programme of drug discovery, which led to the approval in 2009 of Agomelatin® as a treatment for depression (Kasper *et al.*, 2010).

Biphasic saturation and competition curves are not unknown, and have already been described for GPCRs. Biphasic curves using 2-[^{125}I]-melatonin and double-affinity states have already been described in competition tests with melatonin, 2-iodo-melatonin (Witt-Enderby and Dubocovich, 1996), some melatoninergic compounds (Depreux *et al.*, 1994) and guanyl nucleotides (Ying and Niles, 1991; Nonno *et al.*, 1998). Most importantly, these studies were conducted on native tissues such as retina (Dubocovich, 1995), chick brain (Ying and Niles, 1991) and pars tuberalis (Depreux *et al.*, 1994). It is important to note that most of these tissues and organs express both MT_1 and MT_2 receptors (Morgan *et al.*, 1994; Jockers *et al.*, 2008; Dubocovich *et al.*, 2010), which can potentially be responsible for the detection of different binding sites. In the case of Witt-Enderby and Dubocovich (1996), dose–response experiments were run on intact and lysed whole cells (pK_I values of 11.2 and 8.7, respectively); the sensitivity of the first site to GTPγS induced a conversion of the 'super-high' affinity site into the 'high'-affinity site. The 'super-high' affinity IC_{50} was more in the range of hMT_1 affinity as currently described in the literature, whereas the 'high'-affinity state was in a nanomolar range (IC_{50} = 2.0 ± 0.47 nM) that is 1 log lower than our data (Tables 4 and 5); these conversions failed to appear in our saturation curves (Figure 5). Similar experiments were conducted by Nonno *et al.* in 1998 on the Mel_{1a} receptor (i.e.

Table 4

Binding affinities of reference ligands to hMT_1 and hMT_2 receptors as measured with either [^{3}H]-melatonin ([^{3}H]-MLT) or 2-[^{125}I]-melatonin (2-[^{125}I]-MLT)

	hMT_1		hMT_2	
	$pK_i \pm$ SEM	$pK_i \pm$ SEM	$pK_i \pm$ SEM	$pK_i \pm$ SEM
	[^{3}H]-MLT	2-[^{125}I]-MLT	[^{3}H]-MLT	2-[^{125}I]-MLT
MLT	10.15 ± 0.12	9.65 ± 0.02	9.67 ± 0.26	9.27 ± 0.02
2-I-MLT	12.12 ± 0.20	10.71 ± 0.08	11.40 ± 0.18	9.83 ± 0.03
4P-P-DOT	7.56 ± 0.16	6.85 ± 0.04	9.07 ± 0.51	8.97 ± 0.05
Luzindole	8.09 ± 0.31	6.59 ± 0.01	7.80 ± 0.17	7.57 ± 0.01
Ramelteon	11.82 ± 0.06	10.10 ± 0.09	11.52 ± 0.14	10.30 ± 0.19
SD6	11.33 ± 0.34	9.94 ± 0.01	11.33 ± 0.13	9.89 ± 0.22
6-Cl-MLT	9.25 ± 0.07	8.73 ± 0.03	10.09 ± 0.24	9.56 ± 0.12
2-Br-MLT	12.11 ± 0.08	10.82 ± 0.13	11.47 ± 0.23	9.94 ± 0.12
S 70254	7.32 ± 0.31	7.03 ± 0.09	8.31 ± 0.50	9.04 ± 0.08
SD1881 (6-I-MLT)	6.83 ± 0.24	8.84 ± 0.01	8.64 ± 0.14	8.61 ± 0.04
SD1882 (4-I-MLT)	7.95 ± 0.07	7.76 ± 0.12	8.04 ± 0.14	7.99 ± 0.14
SD1918 (7-I-MLT)	7.88 ± 0.10	7.34 ± 0.15	7.53 ± 0.52	7.32 ± 0.15
S 22153	8.25 ± 0.09	8.24 ± 0.14	8.47 ± 0.44	8.01 ± 0.09
S 27128-1	9.03 ± 0.12	8.92 ± 0.01	9.40 ± 0.26	9.17 ± 0.06
Agomelatine	10.17 ± 0.25	9.92 ± 0.01	11.21 ± 0.17	9.93 ± 0.06
D600 (+/–)	7.76 ± 0.15	7.04 ± 0.02	<5	<5
DIV00880	7.44 ± 0.12	6.10 ± 0.04	8.08 ± 0.34	8.04 ± 0.06
5HT	<5	<5	<5	<5
S 20928	7.27 ± 0.26	7.10 ± 0.08	7.65 ± 0.28	7.05 ± 0.25
S 75436	8.53 ± 0.06	7.88 ± 0.01	9.68 ± 0.11	8.87 ± 0.15
S 21278	7.71 ± 0.14	6.22 ± 0.10	7.78 ± 0.22	6.22 ± 0.03
S 73893	8.60 ± 0.06	8.36 ± 0.16	8.90 ± 0.09	8.11 ± 0.23
S 77834	7.87 ± 0.15	7.09 ± 0.05	8.51 ± 0.19	8.53 ± 0.06
S 77840	8.16 ± 0.11	6.15 ± 0.08	7.98 ± 0.05	7.71 ± 0.15

Experiments were conducted using recombinant receptors expressed in CHO-K1 cells. Data are given as mean ± SEM. 4P-P-DOT, 4-phenyl-2-propionamidotetraline.

MT_1). Our use of 2-[^{125}I]-melatonin did not reveal biphasic curves, which is in accordance with the majority of the published data. This 'single-site' profile was confirmed by our kinetics experiments, also in accordance with published data (Kennaway and Hugel, 1992; Witt-Enderby and Dubocovich, 1996) report on hMT_1 and hMT_2 receptors indicated one-parameter kinetic association. [^{3}H]-melatonin kinetics exhibited biphasic curves that are in accordance with saturation experiments, with similar pK_D values. Only hMT_1 receptors at 37°C failed to show two-parameter association kinetics, which can be explained by the very fast association of the radioligand with this receptor. Our kinetics results contrast with the kinetic association studies of Browning *et al.* (2000). Our one-parameter profile can be explained by the density of kinetic points in the fast-association part of the curve. With only three points in this phase, these profiles can be sensitive enough to discriminate two association phases, as is probably the case for our hMT_1 data at 37°C.

[^{3}H]-melatonin allows confirmation of the hypothesis that melatonin receptors are spontaneously coupled to G-proteins

Our approach allowed us to demonstrate that melatonin receptors display two binding sites, as shown by [^{3}H]-melatonin saturation studies conducted under a variety of experimental conditions encompassing inter-species differences in receptor sequence as well as differences in host cell, binding to cell membranes and binding to live cells. We recently reported that when expressed in recombinant systems, melatonin receptors undergo constitutive coupling to G-proteins (Devavry *et al.*, 2012b). We therefore hypothesized that the two sites we report here were comparable to two states of receptor activation. Using GTPγS and NaCl as uncoupling agents (Birnbaumer *et al.*, 1990; Nonno *et al.*, 1998), we were able to convert the high-affinity site (site 1) into the lower-affinity site (site 2). We therefore conclude that

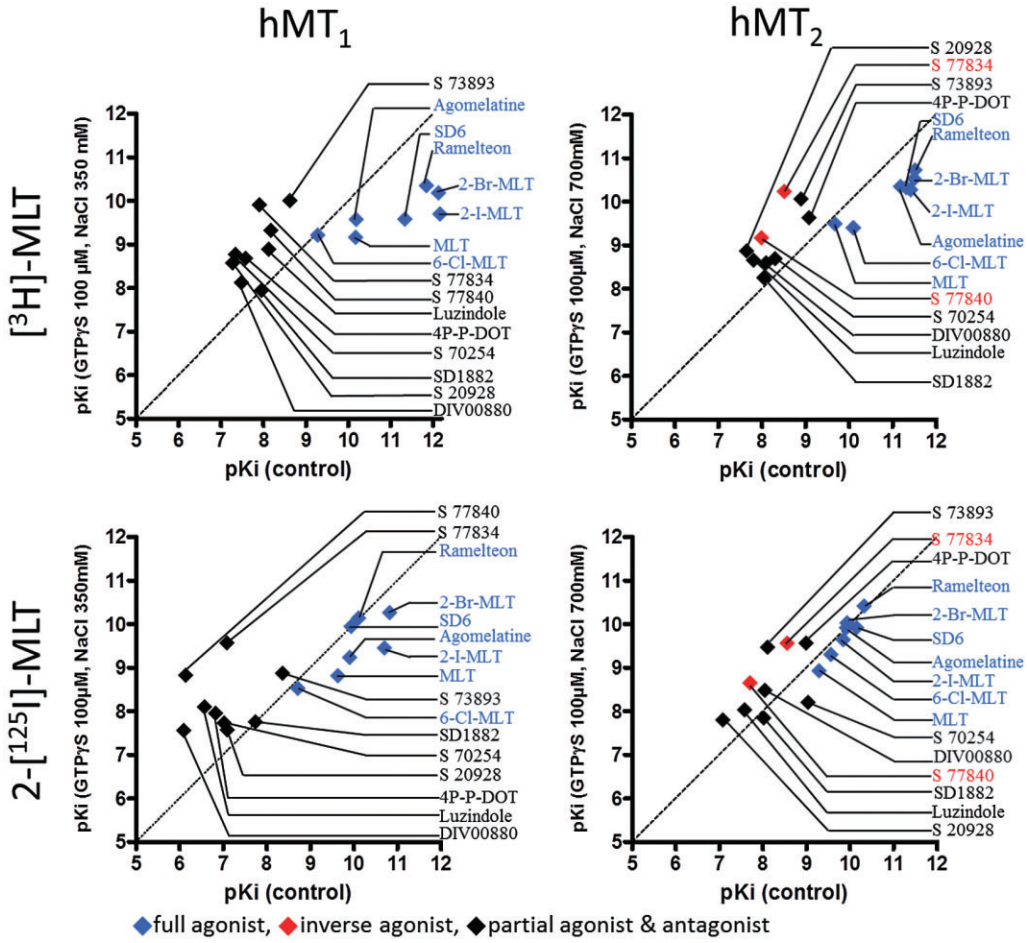

Figure 7

Correlation plot of binding affinities [expressed as $pK_I = -\log(K_I)$] determined for [^{3}H]-melatonin ([^{3}H]-MLT) or 2-[^{125}I]-melatonin (2-[^{125}I]-MLT; from reference database) binding to hMT_1 and hMT_2 receptors in membrane preparations in the presence of 100 µM GTPγS and 350 mM NaCl for hMT_1 and 700 mM NaCl for hMT_2.

the two binding sites observed in [^{3}H]-melatonin saturation studies correspond to the coupled and uncoupled states of the receptor. Interestingly, saturation data indicated that human and ovine receptors have similar properties, while murine receptors may be slightly less responsive to agonists, with higher pK_D values for both the coupled and uncoupled states and a higher proportion of precoupled receptors. It is interesting to consider this observation in the perspective of rat and mouse functional pharmacology, which demonstrates that agonists have 0.5–2.0 log units of difference between murine and human pEC_{50} values, with a higher potency for human receptors (Audinot *et al.*, 2008; Devavry *et al.*, 2012a).

Interestingly, saturation studies of 2-[^{125}I]-melatonin revealed a single binding site for melatonin receptors, as described in this study and as reported most frequently (Reppert *et al.*, 1994; Nonno *et al.*, 1998; 1999; Audinot *et al.*, 2003; Mailliet *et al.*, 2004). This observation suggests that melatonin, but not 2-iodo-melatonin, is able to bind melatonin receptors in both the coupled and uncoupled states. However, this hypothesis is incompatible with our observation that both ligands have sub-nanomolar dissociation constants for [^{3}H]-melatonin and 2-[^{125}I]-melatonin on the MT_1 and MT_2 receptors, with the receptors mostly coupled (native state) or uncoupled (after GTPγS and NaCl treatment; see pK_I values in Table 5). The explanation of this apparent discrepancy resides in the experimental difficulty of working with 2-[^{125}I]-melatonin at concentrations above 1 nM. Our data show that this radioligand has very slow kinetics of association, but is unstable during longer incubations. Therefore, the data obtained in the present investigation result from the balance between the pharmacological properties of the radioligand and the relative instability of the radioligand. As a consequence, the pK_I of 2-iodo-melatonin obtained against [^{3}H]-melatonin differs substantially from its pK_D: pK_I = 12.12 and pK_{D1} = 10.56 for hMT_1 and pK_I = 11.40 and pK_{D1} = 10.11 for hMT_2 (Table 3). Another visible consequence of the instability of 2-[^{125}I]-melatonin during binding experiments is the difference in the pK_I of 2-iodo-melatonin between competition experiments against [^{3}H]-melatonin (pK_I = 12.14 for hMT_1 and pK_I = 11.44 for hMT_2) and against 2-[^{125}I]-melatonin (pK_I = 10.42 for hMT_1 and pK_I = 9.79 for hMT_2). Interestingly, the chemically related ligand 2-

Table 5

Binding affinities of reference compounds to hMT_1 and hMT_2 receptors in the presence of GTPγS and NaCl

	hMT_1		hMT_2	
	GTPγS 100 μM + NaCl 350 mM		GTPγS 100 μM + NaCl 700 mM	
	pK_i ± SEM	pK_i ± SEM	pK_i ± SEM	pK_i ± SEM
	[^{3}H]-MLT	2-[^{125}I]-MLT	[^{3}H]-MLT	2-[^{125}I]-MLT
MLT	9.17 ± 0.23	8.82 ± 0.34	9.48 ± 0.21	8.94 ± 0.25
2-I-MLT	9.72 ± 0.54	9.48 ± 0.45	10.28 ± 0.17	9.64 ± 0.26
4P-P-DOT	8.69 ± 0.12	7.96 ± 0.26	9.63 ± 0.75	9.56 ± 0.03
Luzindole	8.91 ± 0.23	8.11 ± 0.21	8.65 ± 0.18	8.05 ± 0.03
Ramelteon	10.35 ± 0.26	10.14 ± 0.24	10.72 ± 0.34	10.42 ± 0.08
SD6	9.60 ± 0.41	9.95 ± 0.22	10.34 ± 0.28	9.93 ± 0.22
6-Cl-MLT	9.21 ± 0.27	8.53 ± 0.21	9.39 ± 0.49	9.31 ± 0.04
2-Br-MLT	10.20 ± 0.46	10.25 ± 0.27	10.53 ± 0.11	10.00 ± 0.09
S 70254	8.76 ± 0.70	7.73 ± 0.36	8.70 ± 0.47	8.22 ± 0.12
SD1882 (4-I-MLT)	7.97 ± 0.07	7.76 ± 0.42	8.26 ± 0.31	7.86 ± 0.08
Agomelatine	9.56 ± 0.32	9.26 ± 0.18	10.34 ± 0.34	9.93 ± 0.09
DIV00880	8.13 ± 0.23	7.56 ± 0.22	8.58 ± 0.21	8.49 ± 0.08
S 20928	8.60 ± 0.31	7.59 ± 0.19	8.85 ± 0.38	7.80 ± 0.09
S 73893	10.01 ± 0.19	8.89 ± 0.19	10.06 ± 0.22	9.48 ± 0.11
S 77834	9.92 ± 0.37	9.58 ± 0.25	10.23 ± 0.00	9.58 ± 0.03
S 77840	9.32 ± 0.12	8.82 ± 0.31	9.17 ± 0.24	8.66 ± 0.03

Experiments were conducted as described in Methods, using membranes from stably transfected CHO-K1 cells and in the presence of GTPγS and NaCl under standard conditions, using [^{3}H]-melatonin ([^{3}H]-MLT) or 2-[^{125}I]-melatonin (2-[^{125}I]-MLT). Experiments are presented as mean ± SEM for at least three experiments. 4P-P-DOT, 4-phenyl-2-propionamidotetraline.

bromomelatonin also shows this difference of 1.5 log units between pK_I values obtained with the two radioligands (Table 3).

[^{3}H]-melatonin exhibited cooperative binding to MT_1 and MT_2 receptors at low concentrations (data not shown). Cooperative binding requires that the ligand is able to access at least two different binding sites. The binding of the ligand to one site decreases its pK_D for the second site, hence potentiating its recruitment to the protein. In practice, receptor dimerization is the most probable hypothesis for a GPCR to display cooperative binding. Melatonin receptors have been described to form homodimers (Ayoub *et al.*, 2002; 2004), which may explain the cooperative binding observed with [^{3}H]-melatonin. At this point, we have no hypothesis for why 2-[^{125}I]-melatonin does not display such behaviour, but we are currently conducting studies of the heterodimerization of melatonin receptors, which should help understand how it may be linked to cooperative binding of melatonin, but not 2-iodo-melatonin.

To what extent do the MT_1 and MT_2 receptors differ?

It is important to outline the difference in behaviour of hMT_1 and hMT_2 receptors regarding coupled-to-uncoupled conversion using GTPγS and NaCl. These uncoupling agents efficiently converted coupled hMT_2 to a population of uncoupled receptors, with a pK_D value similar to the value that was as part of the natively uncoupled population, as well as a conserved total number of sites. In contrast, upon treatment with uncoupling agents, hMT_1 receptors displayed a few inconsistencies that differed depending on the radioligand used. With [^{3}H]-melatonin, the total number of binding sites was conserved, but the pK_D showed a slight deviation of 0.5 log units from the value anticipated for site 2 under untreated conditions. Conversely, 2-[^{125}I]-melatonin saturation experiments revealed that upon treatment with uncoupling agents, hMT_1 displayed a pK_D in agreement with the overall pattern represented in Figure 6, but most binding sites were lost. Our assay development data indicated that treatment of hMT_1 receptors with either GTPγS or NaCl yielded partial conversion of the receptor population into the uncoupled state (data not shown). Most binding sites were maintained under these conditions, suggesting that while the uncoupling agents used here efficiently uncouple the G-proteins, they are likely also to affect the conformation and the stability of the receptor, obviously with more consequences for hMT_1 than for hMT_2 receptors. This scenario is consistent with our recent difficulty in solubilizing and purifying hMT_1 as compared with other GPCRs, which proved to be less fragile under demanding biochemical conditions.

The pK_D values of [^{3}H]-melatonin and 2-[^{125}I]-melatonin binding to hMT_1 and hMT_2 receptors are presented in sche-

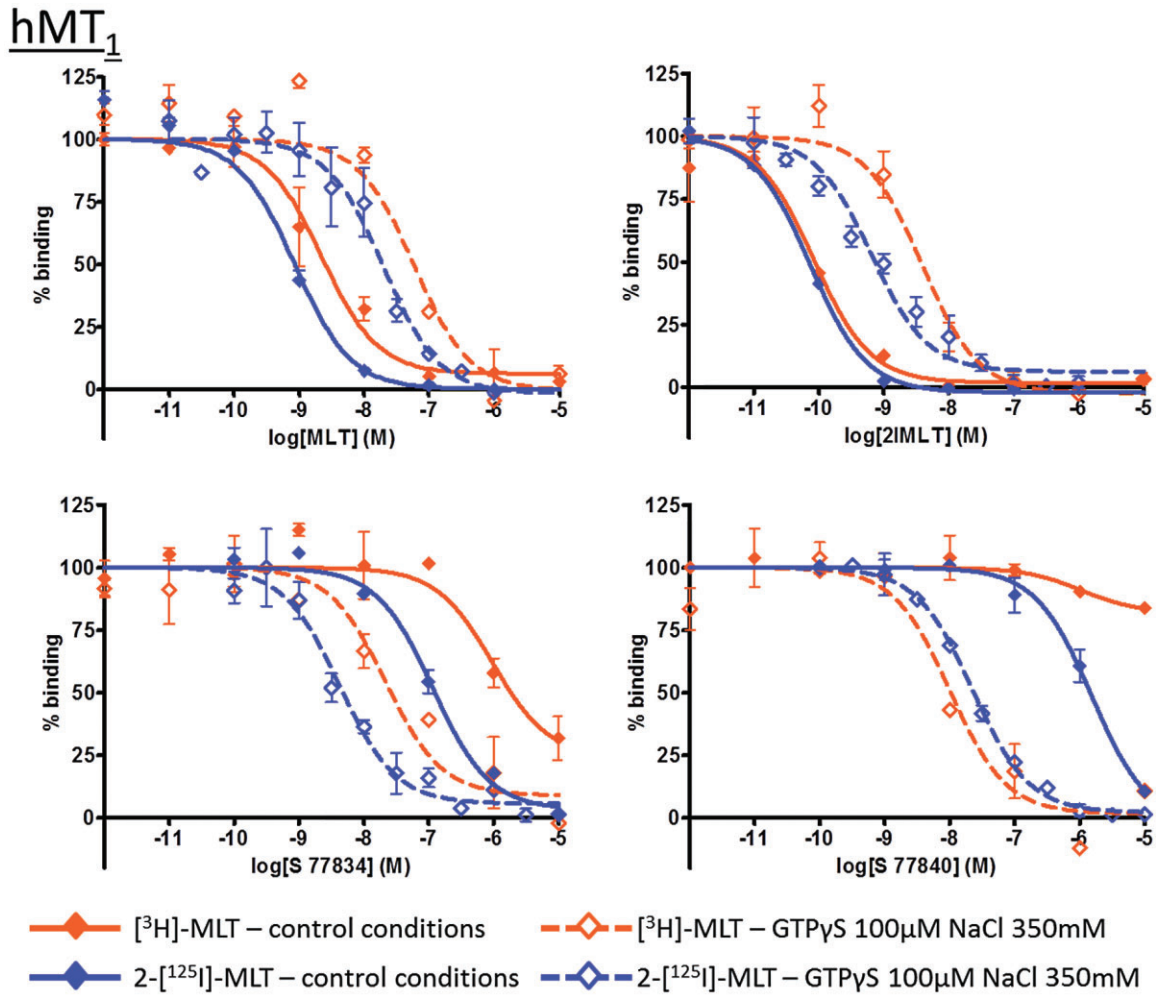

Figure 8

Inhibition curves for melatonin (MLT), 2-iodo-melatonin (2IMLT), S 77834 and S 77840 on hMT_1 receptors with [^{3}H]-MLT and 2-[^{125}I]-MLT, in control condition or in presence of GTPγS 100 µM and NaCl 350 mM. Those individual IC_{50} curves are representative of experiments and illustrate the shift of IC_{50} values but not pK_I in presence of GTPγS and NaCl. Please note that the IC_{50} values suggested by these figures are inherently different from the calculated pK_I values given in the tables and in the text.

matic form in Figure 10, which puts these data into perspective. Although the two radioligands differed in their ability to trace the resting, uncoupled state of the melatonin receptors, the overall pK_D values showed striking overall consistency. The use of uncoupling agents revealed that resting hMT_1 and hMT_2 receptors share the same pK_D for each radioligand. The active, coupled states of two melatonin receptors differed, with hMT_1 having 1 log unit change of pK_D for each radioligand, while hMT_2 showed 0.5 log unit of difference. These data suggest that hMT_1 and hMT_2 receptors have similar pharmacologies as long as they are in the resting state, and that their difference appears, and is revealed, by G-protein coupling. In support of this hypothesis, we observed that the pharmacology of the resting state was well correlated between the two receptors, while the same ligands displayed classical differences in potency (Tables 4 and 5). Similar pK_D values for [^{3}H]-melatonin for the resting-state melatonin receptors were consistently observed across species (human, sheep, mouse and rat). In the coupled state, murine receptors showed a 0.5–1.0-log unit difference in pK_D between the two receptors, similar to that observed with human receptors. Additionally, ovine receptors and human receptors expressed in a neuronal cell line displayed similar pK_D values, suggesting that in these cases, and perhaps *in vivo*, the melatonin receptor subtypes do not significantly differ in their ability to recognize their natural ligand.

Finally, we documented our model of coupled and uncoupled hMT receptors with a set of ligands possessing various functional properties, as assessed by [^{35}S]-GTPγS binding in previous studies (Ersahin *et al.*, 2002; Devavry *et al.*, 2012b). Interestingly, the inverse agonists tended to display a strong bias toward the uncoupled state, with a 1.5–2.0-log unit difference in pK_I with the coupled state of the receptor. Similarly, agonists tended to exhibit higher pK_I values for the coupled states of hMT_1 and hMT_2 receptors. These two observations are more obvious with hMT_1 than with hMT_2 receptors, and are consistent with the general model of Monod–Wyman–Changeux in which the affinity of a ligand

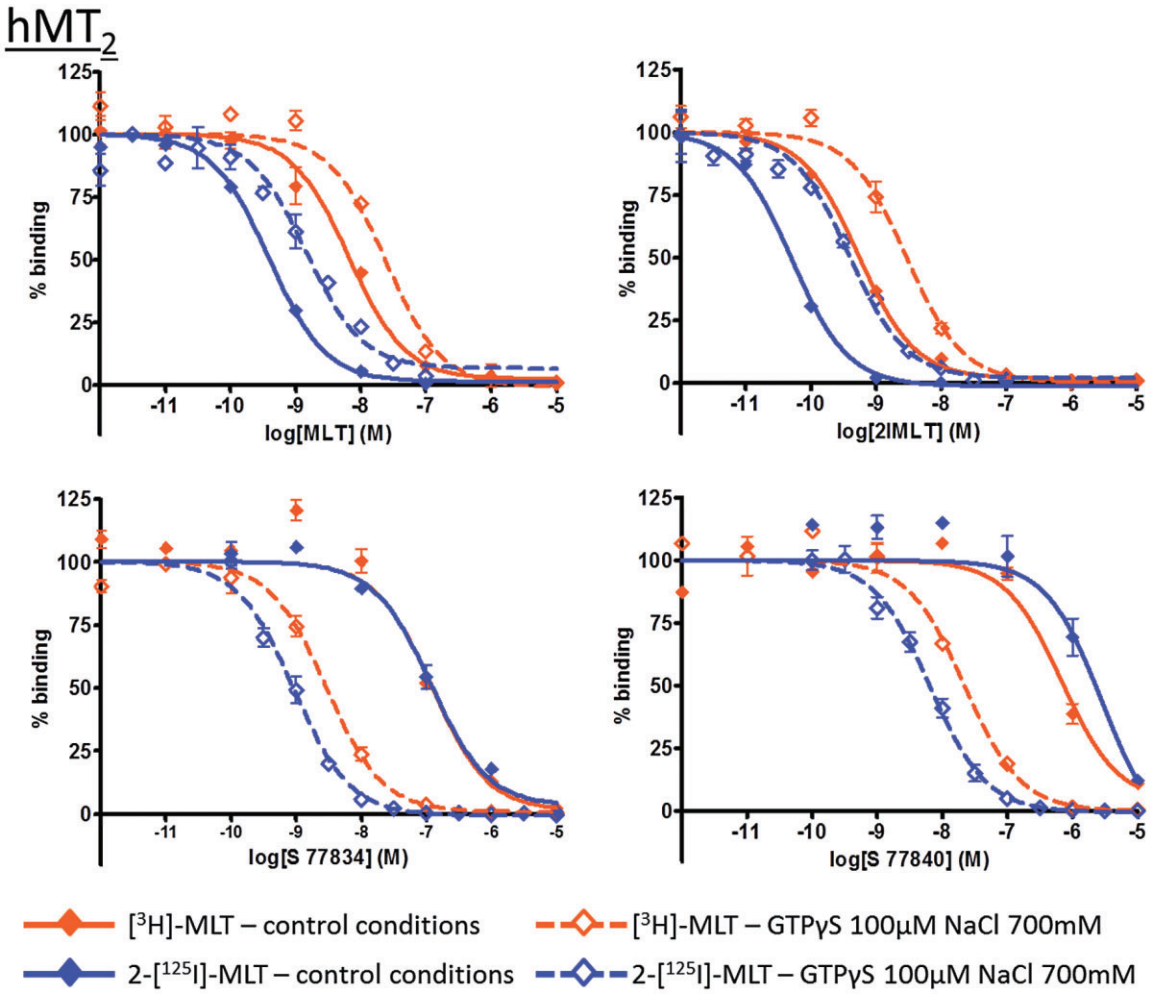

Figure 9

Inhibition curves for melatonin (MLT), 2-iodo-melatonin (2IMLT), S 77834 and S 77840 on hMT_2 receptors with [^{3}H]-MLT and 2-[^{125}I]-MLT, in control condition or in presence of GTPγS 100 μM and NaCl 700 mM. Those individual IC_{50} curves are representative of experiments and illustrate the shift of IC_{50} values but not pK_i in presence of GTPγS and NaCl.

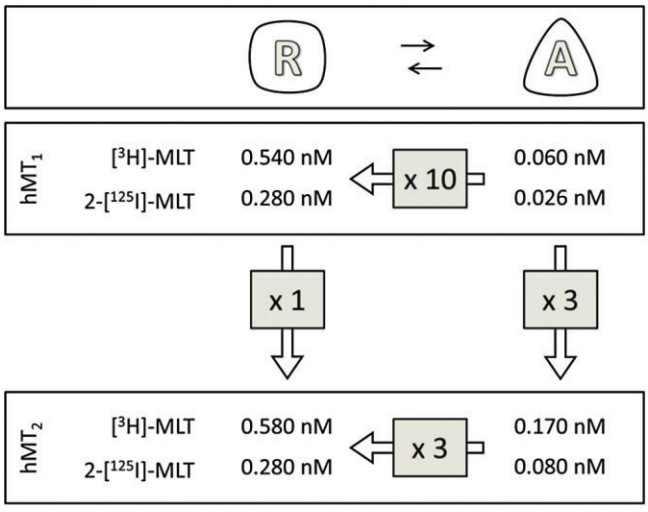

Figure 10

Schematic representation of the various states of melatonin receptors.

for a given state/conformation of a receptor drives the equilibrium of the receptor population to a stabilization of that state, leading agonists to display better affinity to the coupled state of the receptor and inverse agonists to display a better affinity for the uncoupled state.

In conclusion, in this report, we confirm our previous findings that melatonin receptors expressed in heterologous systems undergo spontaneous coupling and reside under a pre-activated conformation in the membrane. As a consequence, the molecular pharmacology described in these models is that of the coupled receptor. The radioligand [^{3}H]-melatonin proved to be instrumental in this study; despite the advantages of 2-[^{125}I]-melatonin in terms of sensitivity, the tritiated physiological ligand proved to be more relevant to fully describe the molecular pharmacology of the melatonin receptors as this radioligand is identical in its chemical structure to the endogenous receptor ligand and as it is able to bind both states, activated or not, of the GPCRs, a feature not seen with 2-[^{125}I]-MLT. We attempted, in this work, to investigate the coupling state of the melatonin receptors in a physiological environment, but despite our expertise in the

preparation of *pars tuberalis*, the very low number of sites (30–60 fmol·mg^{-1}; Piketty and Pelletier, 1993) and the difficulty in obtaining this region did not allow us complete that investigation. The *in vivo* relevance of our observations therefore must be addressed in the future.

Conflict of interests

None.

References

Acuna-Castroviejo D, Reiter RJ, Menendez-Pelaez A, Pablos MI, Burgos A (1994). Characterization of high-affinity melatonin binding sites in purified cell nuclei of rat liver. J Pineal Res 16: 100–112.

Alexander SPH *et al.* (2013). The Concise Guide to PHARMACOLOGY 2013/14: Overview. Br J Pharmacol 170: 1449–1867.

Audinot V, Mailliet F, Lahaye-Brasseur C, Bonnaud A, Le Gall A, Amosse C *et al.* (2003). New selective ligands of human cloned melatonin MT1 and MT2 receptors. Naunyn Schmiedebergs Arch Pharmacol 367: 553–561.

Audinot V, Bonnaud A, Grandcolas L, Rodriguez M, Nagel N, Galizzi JP *et al.* (2008). Molecular cloning and pharmacological characterization of rat melatonin MT1 and MT2 receptors. Biochem Pharmacol 75: 2007–2019.

Ayoub MA, Couturier C, Lucas-Meunier E, Angers S, Fossier P, Bouvier M *et al.* (2002). Monitoring of ligand-independent dimerization and ligand-induced conformational changes of melatonin receptors in living cells by bioluminescence resonance energy transfer. J Biol Chem 277: 21522–21528.

Ayoub MA, Levoye A, Delagrange P, Jockers R (2004). Preferential formation of MT1/MT2 melatonin receptor heterodimers with distinct ligand interaction properties compared to MT2 homodimers. Mol Pharmacol 66: 312–321.

Birnbaumer L, Abramowitz J, Brown AM (1990). Receptor-effector coupling by G proteins. Biochim Biophys Acta 1031: 163–224.

Bradford MM (1976). A rapid and sensitive method for the quantitation of microgram quantities of protein utilizing the principle of protein-dye binding. Anal Biochem 72: 248–254.

Browning C, Beresford I, Fraser N, Giles H (2000). Pharmacological characterization of human recombinant melatonin mt(1) and MT(2) receptors. Br J Pharmacol 129: 877–886.

Cheng YC, Prussof WH (1973). Relationship between the inhibition constant (K_i) and the concentration of inhibitor which causes 50% inhibition (IC_{50}) of an enzymatic reaction. Biochem Pharmacol 22: 3099–3108.

Cogé F, Guenin SP, Fery I, Migaud M, Devavry S, Slugocki C *et al.* (2009). The end of a myth: cloning and characterization of the ovine melatonin MT(2) receptor. Br J Pharmacol 158: 1248–1262.

Depreux P, Lesieur D, Mansour HA, Morgan P, Howell HE, Renard P *et al.* (1994). Synthesis and structure-activity relationships of novel naphthalenic and bioisosteric related amidic derivatives as melatonin receptor ligands. J Med Chem 37: 3231–3239.

Devavry S, Legros C, Brasseur C, Cohen W, Guenin SP, Delagrange P *et al.* (2012a). Molecular pharmacology of the mouse melatonin receptors MT(1) and MT(2). Eur J Pharmacol 677: 15–21.

Devavry S, Legros C, Brasseur C, Delagrange P, Spadoni G, Cohen W *et al.* (2012b). Description of the constitutive activity of cloned human melatonin receptors hMT(1) and hMT(2) and discovery of inverse agonists. J Pineal Res 53: 29–37.

Drew JE, Barrett P, Mercer JG, Moar KM, Canet E, Delagrange P *et al.* (2001). Localization of the melatonin-related receptor in the rodent brain and peripheral tissues. J Neuroendocrinol 13: 453–458.

Dubocovich ML (1995). Melatonin receptors: are there multiple subtypes? Trends Pharmacol Sci 16: 50–56.

Dubocovich ML, Delagrange P, Krause DN, Sugden D, Cardinali DP, Olcese J (2010). International Union of Basic and Clinical Pharmacology. LXXV. Nomenclature, classification, and pharmacology of G protein-coupled melatonin receptors. Pharmacol Rev 62: 343–380.

Ersahin C, Masana MI, Dubocovich ML (2002). Constitutively active melatonin MT(1) receptors in male rat caudal arteries. Eur J Pharmacol 439: 171–172.

Ettaoussi M, Sabaouni A, Pérès B, Landagaray E, Nosjean O, Boutin JA *et al.* (2013). Synthesis and pharmacological evaluation of a series of the agomelatine analogues as melatonin MT_1 /MT_2 agonist and 5-HT_{2C} antagonist. ChemMedChem. in press

Jockers R, Maurice P, Boutin JA, Delagrange P (2008). Melatonin receptors, heterodimerization, signal transduction and binding sites: what's new? Br J Pharmacol 154: 1182–1195.

Kasper S, Hajak G, Wulff K, Hoogendijk WJ, Montejo AL, Smeraldi E *et al.* (2010). Efficacy of the novel antidepressant agomelatine on the circadian rest–activity cycle and depressive and anxiety symptoms in patients with major depressive disorder: a randomized, double-blind comparison with sertraline. J Clin Psychiatry 71: 109–120.

Kennaway DJ, Hugel HM (1992). Melatonin binding sites: are they receptors? Mol Cell Endocrinol 88: C1–C9.

Kennaway DJ, Hugel HM, Rowe SA (1994). Characterization of the chicken brain melatonin-binding protein using iodinated and tritiated ligands. J Pineal Res 17: 137–148.

Legros C, Matthey U, Grelak T, Pedragona-Moreau S, Hassler W, Yous S *et al.* (2013). New radioligands for describing the molecular pharmacology of MT_1 and MT_2 melatonin receptors. Int J Mol Sci 14: 8948–8962.

Mailliet F, Audinot V, Malpaux B, Bonnaud A, Delagrange P, Migaud M *et al.* (2004). Molecular pharmacology of the ovine melatonin receptor: comparison with recombinant human MT1 and MT2 receptors. Biochem Pharmacol 67: 667–677.

Masana MI, Dubocovich ML (2001). Melatonin receptor signaling: finding the path through the dark. Sci STKE 2001: PE39.

Mazzucchelli C, Pannacci M, Nonno R, Lucini V, Fraschini F, Stankov BM (1996). The melatonin receptor in the human brain: cloning experiments and distribution studies. Brain Res Mol Brain Res 39: 117–126.

Morgan PJ, Barrett P, Howell HE, Helliwell R (1994). Melatonin receptors: localization, molecular pharmacology and physiological significance. Neurochem Int 24: 101–146.

Niles LP (1987). [3H] melatonin binding in membrane and cytosol fractions from rat and calf brain. J Pineal Res 4: 89–98.

Nonno R, Lucini V, Pannacci M, Mazzucchelli C, Angeloni D, Fraschini F *et al.* (1998). Pharmacological characterization of the

human melatonin Mel1a receptor following stable transfection into NIH3T3 cells. Br J Pharmacol 124: 485–492.

Nonno R, Fraschini F, Stankov BM (1999). Methods for the evaluation of drug action at the human melatonin receptor subtypes. Biol Signals Recept 8: 32–40.

Piketty V, Pelletier J (1993). Melatonin receptors in the lamb pars tuberalis/median eminence throughout the day. Neuroendocrinology 58: 359–365.

Reppert SM, Weaver DR, Ebisawa T (1994). Cloning and characterization of a mammalian melatonin receptor that mediates reproductive and circadian responses. Neuron 13: 1177–1185.

Reppert SM, Godson C, Mahle CD, Weaver DR, Slaugenhaupt SA, Gusella JF (1995). Molecular characterization of a second melatonin receptor expressed in human retina and brain: the Mel1b melatonin receptor. Proc Natl Acad Sci U S A 92: 8734–8738.

Vakkuri O, Lamsa E, Rahkamaa E, Ruotsalainen H, Leppaluoto J (1984). Iodinated melatonin: preparation and characterization of the molecular structure by mass and 1H NMR spectroscopy. Anal Biochem 142: 284–289.

Williams LM, Hannah LT, Hastings MH, Maywood ES (1995). Melatonin receptors in the rat brain and pituitary. J Pineal Res 19: 173–177.

Williams LM, Hannah LT, Bassett JM (1999). Melatonin receptors in neonatal pig brain and pituitary gland. J Pineal Res 26: 43–49.

Witt-Enderby PA, Dubocovich ML (1996). Characterization and regulation of the human ML1A melatonin receptor stably expressed in Chinese hamster ovary cells. Mol Pharmacol 50: 166–174.

Ying SW, Niles LP (1991). 3-[(3-cholamidopropyl) dimethylammonio]-1-propane sulfonate-solubilized binding sites for 2-[125I]iodomelatonin in chick brain retain sensitivity to guanine nucleotides. J Neurochem 56: 580–586.

Zawilska JB, Skene DJ, Arendt J (2009). Physiology and pharmacology of melatonin in relation to biological rhythms. Pharmacol Rep 61: 383–410.

Zlotos DP, Attia MI, Julius J, Sethi S, Witt-Enderby PA (2009). 2-[(2,3-dihydro-1H-indol-1-yl)methyl]melatonin analogues: a novel class of MT2-selective melatonin receptor antagonists. J Med Chem 52: 826–833.